Thermodynamic modelling and energy balance of direct methanation of glycerol for Bio-SNG production

Robert White[a],[*], Valerie Dupont[b], Timothy Cockerill[c]

[a] Centre for Doctoral Training Bioenergy, Faculty of Engineering, University of Leeds, Leeds, United Kingdom
[b] School of Chemical and Process Engineering, Faculty of Engineering, University of Leeds, Leeds, United Kingdom
[c] Centre for Integrated Energy Research, School of Mechanical Engineering, Faculty of Engineering, University of Leeds, Leeds, United Kingdom

ARTICLE INFO

ABSTRACT

Glycerol can be considered a waste product when the cost of processing is higher than the processed glycerol value. In these situations, conversion of glycerol to an energy vector may be more beneficial. The aim of this work was to design and assess the feasibility of a process for low temperature steam reforming of glycerol (GLT-SR). GLT-SR is a novel form of direct methanation that produces a CH_4 rich, renewable fuel gas (Bio-SNG) that could substitute the current natural gas consumption associated with biodiesel production.

In this work, thermodynamic modelling to determine the conditions that suited CH_4 production and mini-mised carbon below 600 K as well as the impact of molar steam to carbon ratio (S/C) and pressure on the biomass to fuel efficiency of a GLT-SR plant were carried out using Aspen Plus® (V8.8) chemical processing software. Operating at 8 atm provided the benefits of high conversion to CH_4 whilst minimising the outlet reformer temperature and achieving the required inlet temperature for catalyst operation.

The Bio-SNG produced had an LHV of 16.7 MJ kg^{-1} and had properties like landfill gas and biogas. An energy balance of the process determined that the electricity demand was negligible due to the low energy use of pumps and fans without the need for compressors. Operating at 8 atm, the production of Bio-SNG in the GLT-SR plant has the potential to offset 30% of the natural gas embodied energy requirement or 8.9% of the total embodied energy requirement for soybean biodiesel production from farm to use.

1. Introduction

Global production of biodiesel and the co-product glycerol have increased in the last two decades [1]. As nations strive to decarbonise transport fuels, global production of biodiesel is forecasted to double from 20 billion litres in 2009 to 41 million litres in 2025 with biodiesel transesterification producing as much as 10 wt% glycerol as a by-product [2].

Typically, glycerol represented an important area of profitability for biodiesel refineries. As production of biodiesel, and therefore glycerol has increased, supply of glycerol has become entirely independent of demand resulting in consistently low glycerol prices [3]. Current low economic value of glycerol in crude and purified forms, as well as the environmental toxicity, increases the pressure on biodiesel refineries as the costs for storage, transport, post treatment and disposal have remained the same. In the UK, as of 2008, where it is not possible to send the crude glycerol for purification or an alternative beneficial use, it must be consigned as waste [4].

Several methods are available to convert glycerol into higher value chemicals or green fuels. He et al., 2017 provides details on these methods when using crude glycerol as a feedstock and includes; fermentation, digestion, gasification, pyrolysis, liquefaction, combustion and steam reforming. The main focus for studies in the area of producing green fuels by thermochemical processes is to produce hydrogen or syngas as the main product by gasification or reforming [5]. Several of these studies combine crude or pure glycerol with another biomass feedstock to enhance the process or act under supercritical or hydro-thermal conditions and are not reviewed in this work.

Techniques for glycerol reforming include steam, partial oxidation, autothermal, aqueous, supercritical water reforming and have been reviewed by Schwengber et al. [6]. In addition sorption enhanced re-forming [7–9] and dry reforming [10] have been reviewed.

Steam reforming (SR) of pure glycerol to produce hydrogen has received significant research emphasis over the last decade. SR of gly-cerol requires the addition of steam to glycerol in a suitable steam to carbon ratio over a catalyst at elevated temperatures. The popularity of the steam reforming process using glycerol feedstock is owed to how well SR has been established at industry level with more abundant and

cheap organic feedstocks such as natural gas. Steam methane reforming is still used today to generate a significant proportion of the world's commercial hydrogen.

Moreover, if glycerol steam reforming processes become viable, minimal modifications will be required for steam methane reforming plants to switch to glycerol feed when compared to the other, less well established techniques such as aqueous phase reforming or supercritical water gasification, which are yet to reach this stage [11].

The main disadvantages of steam reforming when compared to the other reforming methods are the high temperatures, and therefore high energy input, required to vaporise the glycerol and water and provide adequate conditions for syngas and hydrogen production [12].

Steam reforming is mentioned in several different reviews in addition to He et al. [5] and Schwengber et al. [6]. Bagnato et al. [13] presents work on glycerol steam reforming and the main areas of catalyst development with a focus on membrane reactors. Rodrigues et al. [11] describes and compares glycerol steam reforming with carbonation and acylation with an emphasis on catalysis and experimental analysis with a thermodynamics-based discussion of glycerol steam reforming. The overarching theme is that glycerol can become a sustainable source of hydrogen, closing the loop for biodiesel refineries and increasing their profit.

Utilising pure glycerol rather than crude avoids the contaminants from biodiesel transesterification and allows simpler modelling. The majority of glycerol steam reforming studies are based on pure glycerol. Of significant interest for this work are the thermodynamic studies that have been carried out for steam reforming of pure glycerol above 550 K (277 °C) [14–19]. Silva et al. [20] published a review including the thermodynamics of glycerol steam reforming and progress with different catalysts. The focus of the thermodynamic studies is to determine operating conditions that favour H_2 and inhibit CH_4 and carbon (coking) production.

Fewer studies have been carried out using crude glycerol and He et al. 2017 reviews works converting crude glycerol to hydrogen and syngas [5]. In addition to these works production of syngas by noncatalysed steam reforming of crude glycerol by experiment [21] and production of hydrogen by; steam reforming of crude glycerol using nickel supported on activated carbon [22], rhodium over $MgAl_2O_4$ [23] and Ni-La-Ti mixed oxide catalysts [24], and dry autothermal reforming (ATR) of crude glycerol with *in situ* hydrogen separation by thermodynamic modelling [25] have been reported.

A direction that has not yet been fully explored is direct synthesis of methane from waste glycerol at low temperatures and pressures to produce a renewable fuel gas (Bio-SNG). Operating at low temperatures and pressures avoids the high energy costs associated with steam reforming and safety issues with supercritical conditions. Hydrogen is produced during the initial decomposition of glycerol (Eq. (1)) which is readily available for the steam reforming reaction. Carrying out steam reforming of glycerol by direct methanation without additional hydrogen creates an upper theoretical limit on methane production. The theoretical maximum CH_4 that can be produced from one mole of glycerol is shown in Eq. (2) by combining the glycerol decomposition (Eq. (1)), water gas shift (Eq. (3)) and carbon monoxide methanation (Eq. (4)) and was mentioned by Schubert et al. [26]. Whilst the CO_2 methanation pathway in Eq. (5) is possible, it consumes more hydrogen for the same yield of methane and is dependent on the water gas shift reaction for CO_2 production. Carbon formation can inhibit methane production in steam reforming reactions and occurs by disproportionation of CO in Eq. (6) (Boudouard reaction) as well as CO and CO_2 hydrogenation in Eq. (7) and Eq. (8).

Glycerol Decomposition to Syngas

$$C_3H_8O_{3(l)} \xrightarrow{heat} 4H_2 + 3CO \quad \Delta H^0_{298} + 338 \text{ kJ mol}^{-1} \tag{1}$$
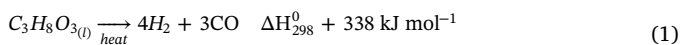
Glycerol Autothermal Reforming (direct methanation of glycerol)

$$C_3H_8O_{3(l)} \rightarrow 1.75CH_4 + 1.25CO_2 + 0.5H_2O \quad \Delta H^0_{298} -74 \text{ kJ mol}^{-1} \tag{2}$$

Water Gas Shift

$$CO + H_2O \leftrightarrows CO_2 + H_2 \quad \Delta H^0_{298} -41 \text{ kJ mol}^{-1} \tag{3}$$

CO Methanation

$$CO + 3H_2 \leftrightarrows CH_4 + H_2O \quad \Delta H^0_{298} -206 \text{ kJ mol}^{-1} \tag{4}$$

CO_2 Methanation

$$CO_2 + 4H_2 \leftrightarrows CH_4 + 2H_2O \quad \Delta H^0_{298} -165 \text{ kJ mol}^{-1} \tag{5}$$
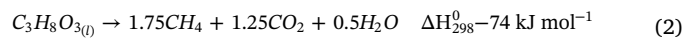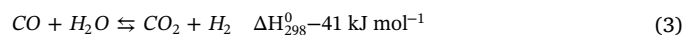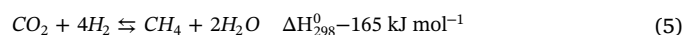
CO Disproportionation (Boudouard)

$$2CO \leftrightarrows CO_2 + C \quad \Delta H^0_{298} -172 \text{ kJ mol}^{-1} \tag{6}$$

CO Hydrogenation

$$CO + 2H_2 \leftrightarrows H_2O + C \quad \Delta H^0_{298} -131 \text{ kJ mol}^{-1} \tag{7}$$

CO_2 Hydrogenation

$$CO_2 + 2H_2 \leftrightarrows 2H_2O + C \quad \Delta H^0_{298} -90 \text{ kJ mol}^{-1} \tag{8}$$
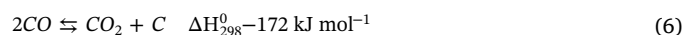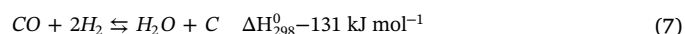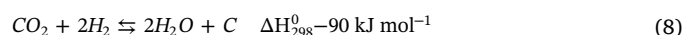
The concept of direct methanation was first recorded by Meyer. H et al. (1976). Meyer described the improvements over the conventional syngas methanation process by reacting equimolar concentrations of CO and H_2 in Eq. (9). Whilst the stoichiometry is the same as combining the CO methanation and water gas shift, the difference was that CO_2 was produced directly rather than by water gas shift [27].

Combined CO methanation and CO Shift

$$2CO + 2H_2 \leftrightarrows CH_4 + CO_2 \quad \Delta H^0_{298} -247 \text{ kJ mol}^{-1} \tag{9}$$
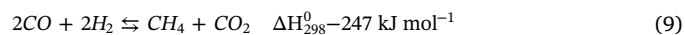
To date, there has been one experimental study on a direct synthesis of methane from glycerol was carried out by Imai Hiroyuki [28]. Silica modified nickel catalysts were used to directly methanate a solution of pure glycerol and water at a steam to carbon ratio of 1.71 (50 wt% glycerol), 1.14 (60 wt% glycerol) and 0.73 (70 wt% glycerol) at temperatures between 593 K and 723 K and pressures of 1–30 atm.

Converting glycerol to methane represents an opportunity to produce a renewable energy carrier that is like biogas or landfill gas and can therefore operate within current gas infrastructures. To minimise economic expenditure the following methods could be applied: effective heat integration to maximise efficiency, install the process on site at biodiesel refineries to minimise transport and logistics costs, minimise power requirements by utilising the Bio-SNG without upgrading and minimise external thermal energy demand by combusting some of the Bio-SNG on site to produce steam and closing the loop.

Producing the Bio-SNG on site at the biodiesel refinery would provide a source of renewable fuel that could substitute natural gas used for heat and power, thereby reducing the refineries dependence on fossil fuel whilst simultaneously preventing waste and improving the energy efficiency of the biodiesel plant. An example of how the Bio-SNG could replace natural gas in a soybean biodiesel refinery is shown in Fig. 1.

Based on the thermodynamic literature, it is widely agreed that favouring CH_4 rather than H_2 production requires low steam to carbon ratios and temperatures with elevated pressures [14,16,29]. More specifically temperatures below 900 K, pressures greater than 1 atm and an S/C above the minimum for negligible solid carbon product but lower than three. Above 950 K CH_4 is almost inhibited due to steam methane reforming at 1 bar [29]. Increasing pressure reduces solid carbon up to 850 K but increases solid carbon formation above 850 K [16]. Reactions that favour solid carbon are: thermal decomposition, cracking, and CO disproportionation (Eq. (6)). Minimising carbon product is integral to prolonging catalyst life and activity in reactors as well as maximising the conversion of glycerol carbon to CH_4.

The minimum temperature for methanation is limited by the activity of catalysts. The minimum temperature advised for the commercial PK-7R low temperature CO methanation catalyst created by
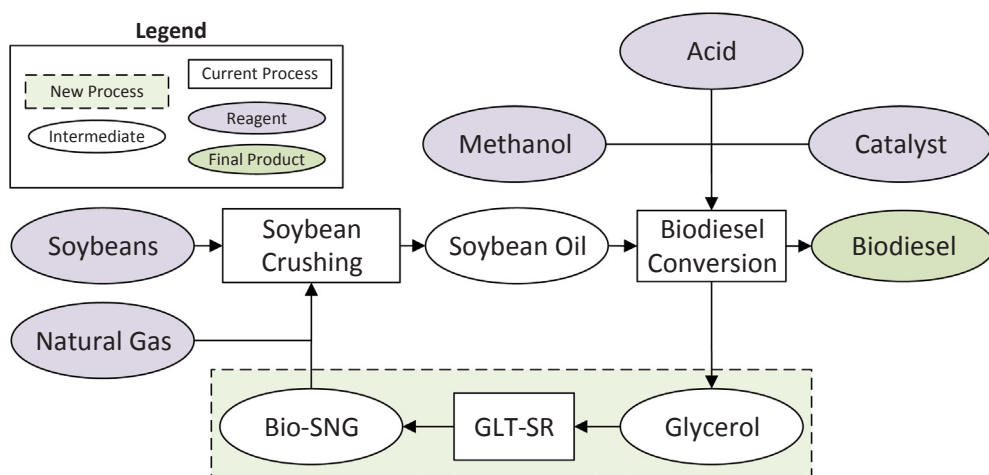
Fig. 1. Simplified block diagram of the proposed integration of GLT-SR into a soybean biodiesel plant. The dotted line highlights the additional GLT-SR process.

Haldor Topsoe is 463 K (190 °C) [30]. Additionally Zhang et al. [31] reports that experimental glycerol conversion to products occurred at 100% at 673–723 K over ceria supported metal catalysts although most thermodynamic models will assume 100% conversion at temperatures of 673 K and below. Pressures to be investigated should be between 1 and 30 atm as this creates only mild stress on the catalyst [32].

The ideal property method has been used by Adhikari et al. [14], Chen et al. [29], Dieuzeide and Amadeo [16], and Rossi et al. [15] whilst the Redlich Kwong equation of state was used by Wang et al. [19] and the solids property method by Tippawan et al. [9]. Glycerol is a polar non-electrolyte compound. Carlson recommends NRTL and UNIQUAC with their variants and Peng Robinson (PENG) and Redlich Kwong (RK) equations of state for systems where data is available [33]. The solids property method acts like the ideal property method when dealing with liquid and vapour phases.

This work proceeds with an investigation into the thermodynamics of direct methanation of glycerol at low temperatures. A plant is designed and the energy efficiency as well as the potential to offset natural gas use in soybean biodiesel refining is analysed. This study serves as the first in a series of studies that will ultimately lead to designing a process that converts crude glycerol into a Bio-SNG by direct methanation.

2. Process modelling

Aspen Plus V8.8 process modelling software was used to gain deeper insight into the thermodynamics of glycerol steam reforming at temperatures below 600 K with a focus on temperature, pressure and steam to carbon ratio variables on CH_4 production. Using this data, a plant was designed that housed a direct catalytic methanation process (steam reformer). The energy efficiencies were calculated and a sensitivity analysis on the heating value and methane content of the Bio-SNG was explored to gain insight into the effects of different process parameters including; operating pressure and temperature, glycerol feed inlet temperature, steam to carbon ratio and furnace efficiency and vapour fractions. The minimum temperature for total vaporisation (vapour fraction = 1) of a water and glycerol mixture can be calculated in Aspen Plus, using the binary mixing analysis mode.

An equilibrium Gibbs Reactor model (RGIBBS) was used to simulate both isothermal and adiabatic low temperature steam reforming of pure glycerol by minimising Gibbs free energy. Pure glycerol characteristics from the NIST database were used. The lower heating value of glycerol was 16.07 MJ kg^{-1}. For the present study, it is assumed that the feedstock is pure (100%) glycerol to avoid the hitherto unpredictable effects of contaminants and to determine the potential of glycerol methanation. The component inputs were conventional except for carbon which was selected as a solid component and is known as carbon graphite.

Components included were; glycerol, CH_4, H_2, CO, CO_2, H_2O, NO, N_2, NO_2 and C and were potential products.

The main input variables were reformer pressure, feed inlet temperature, reformer temperature and property methods. The outputs of interest were: minimum molar steam to carbon ratio for zero carbon product, outlet reactor temperature, and outlet Bio-SNG composition and mass.

A sensitivity analysis was carried out on temperatures 400–100 K and pressures of 1–30 atm with molar steam to carbon ratio (S/C) between 1 and 3. The literature reports thermodynamic simulations for glycerol steam reforming for isothermal conditions under the IDEAL property method with Gibbs free energy minimisation. The main property methods compared in this work were IDEAL, NRTL, NRTL-RK, PENG, and UNIQUAC based on the selection methods by Carlson [33].

The minimum S/C for each temperature to prevent carbon as equilibrium product was the point at which methanation was most favoured, as any additional increase in temperature or S/C hindered the CH_4 yield by increasing the co-product hydrogen. It is noteworthy that steam methane reforming plants usually operate at S/C of 3 across all pressures as this favours H_2 production, even though thermodynamic analysis shows that it is possible to prevent carbon formation at as low as S/C of 1.1 at 10 atm [34].

2.1. Designing a GLT-SR plant

The GLT-SR plant was designed according to Fig. 2. A sensitivity analysis of the variables mentioned in 2.0 on the plant efficiencies and gas LHV was produced.

The glycerol inlet feed was based on the mass of glycerol generated from soybean biodiesel production. It was reported that 3,975,000 kg year^{-1} of soybean glycerol could be produced at a ratio of 0.119 kg L^{-1} biodiesel whereby the biodiesel density was taken as 0.8746 kg L^{-1} from GREET [35,36]. Assuming the GLT-SR plant operates for 8000 h, this led to 497 kg hr^{-1} of glycerol feed.

Glycerol and steam were fed to the adiabatic RGIBBS reformer and converted to gas. The gas was fed through a series of four heat exchangers and 1 condenser. H1 and H2 recycled heat to produce steam for use in the reforming process using water that was condensed out of the gas later in C1. H3 pre-heated air for the furnace and H4 recycled the remaining heat to produce low pressure steam. C1 removed water from the gas and it was assumed that all the H_2O could be condensed and removed from the gas without the loss of CH_4 or CO_2 in the condensate. The pressure drop associated with the outlet of any stream passing through a heat exchangers was assumed 10% of the inlet value.

A fraction of the gas was recirculated to the RGIBBS *furnace* in the stream RE-BG and combusted with 10% excess air. This provided the remaining energy for steam generation which was carried out in the
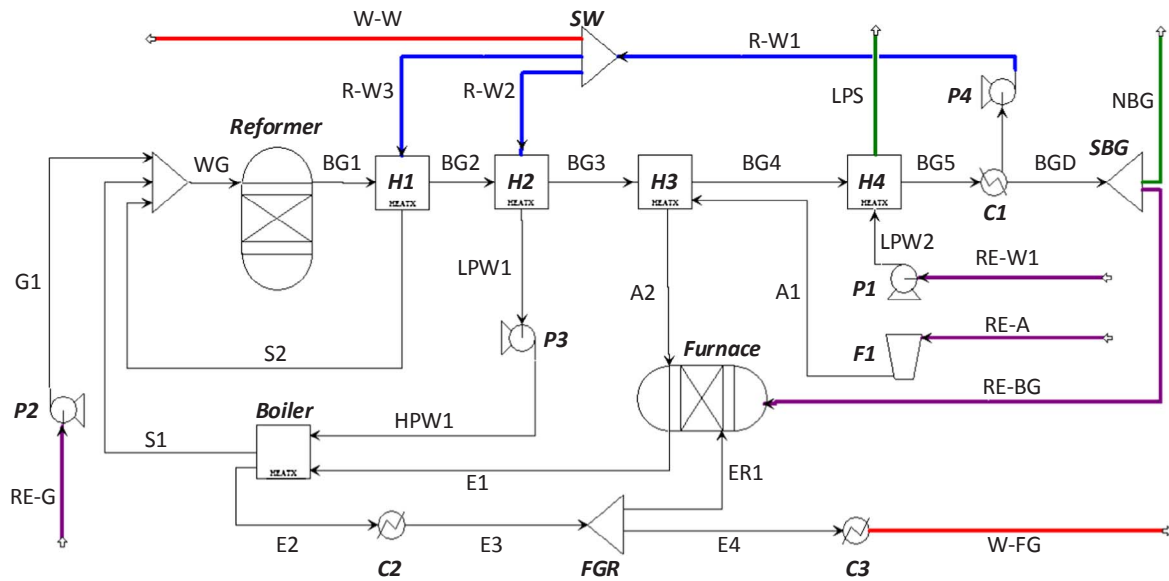
Fig. 2. Aspen Plus V8.8 process flow sheet for GLT-SR. Burgundy streams with notation 'RE' are feed inlets, blue streams with notation 'R' are recycled water, red streams with notation 'W' are waste outlets and green streams are product outlets. Italicised and emboldened labels are blocks whereas standard font are streams. A = air, BG = Bio-SNG, BGD = Dry Bio-SNG, C = cooler, E = exhaust, F = fan, FG = flue gas, FGR flue gas recirculation, G = glycerol, H = heat exchanger, HPW = high pressure water, LPW = low pressure water, LPS = low pressure steam, P = pump, S = steam, SBG = splitter Bio-SNG, SW = splitter water, WG = water glycerol. (For interpretation of the references to colour in this figure legend, the reader is referred to the web version of this article.)

Boiler. The *furnace* was assumed to have a heat transfer efficiency of 90% [37] and was achieved by adding a negative heat duty equal to 10% of the total positive heat duty produced by combustion of Bio-SNG. A fraction of the exhaust was recirculated to the *furnace* by the stream ER1 to maintain an exhaust temperature in E1 of 1315 °C (1588 K), with a tolerance of 5 °C. The water content in the exhaust was 16.7% mf, which fell within the range of 5.7–19.4% for flue gas recirculation in Liuzzo et al.'s [38] simulations for incineration. A fan was represented by F1 and was used to drive the combustion air to the furnace whilst pumps were used to circulate glycerol and water. The pumps efficiencies were 29.6% whilst the fan was modelled as an isentropic compressor with 72% efficiency and allowed the power input of the process to be recorded. Aspen plus calculated all heating values by low heating value.

2.2. Calorific value

The calorific value 'HHV_G' bio-SNG as determined using Eq. (10).

$$HHV_G = \sum y_i HHV_i \tag{10}$$

where HHV_g was the higher heating value of the Bio-SNG (J mol^{-1}), y was the gas mole fraction, i was the gas component, and HHV_i was the higher heating value of the component. Eq. (10) was also used for lower heating value 'LHV' calculations used in the efficiencies calculations in 2.3. The reference temperature for combustion for heating values was 15 °C and the reference temperature and pressure for standard density and volume for heating value were 15 °C and 1 atm.

2.3. Energy and efficiencies

Gibbs free energy was calculated according to Eq. (11) using standard heats of formation, enthalpy and entropy for the water gas shift, CO methanation and CO_2 methanation.

$$\Delta G^o = \Delta H^o - T\Delta S^o \tag{11}$$

G is Gibbs free energy, H is enthalpy of formation, T is temperature and S is standard entropy.

The calculations of energy and efficiencies were based on the plant and process diagram of the GLT-SR process as shown in Fig. 2. The

pumps, compressors, heat exchangers, condenser, furnace and reformer all provided heat and power duties which were used to determine the energy balance.

To calculate the energy required for pumping fluids a form of the Bernoulli equation was used, as shown in Eq. (12).

$$w = m\left[\frac{\Delta p}{\rho} + \frac{du}{At} + g\Delta z + gh_L\right] \tag{12}$$

where w was work done, m was mass of incompressible fluid being pumped, Δp was the change in pressure between the inlet of the fluid and outlet of the fluid, ρ was the density of the fluid, d was the distance the fluid must travel, u was the fluid flow rate or speed, A was the cross-sectional area of the pipe, t was the time required for the fluid to reach its destination, g was the acceleration of gravity, Δz was the change in height and h_L was the head loss calculated from the friction, diameter and velocity. Assumed values for pipe distance was 20 m, pipe radius was 0.2 m, height was 20 m and friction coefficient was 0.1. These values were used to provide an alternative estimate of the work done, as Aspen plus V8.8 assumed by default that the kinetic energy was negligible and the change in height was zero. The efficiency of the pump was 0.296 and a pressure increase of 0.5 atm was used to generate flow.

To calculate the energy for fans Eq. (13) was used:

$$w = m \cdot q_{out} + m(h_2 - h_1) \tag{13}$$

where w was work done by the compressor or fan, m was the mass of the gas being compressed, q_{out} was the heat loss, h_2 was the enthalpy of the gas after compression and h_1 was the enthalpy of the gas before compression. Aspen Plus V8.8 did not utilise a heat loss coefficient and this value was also left as zero for the energy balance calculations. The settings in Aspen Plus V8.8 were isentropic compression with an efficiency of 0.73.

The temperature of the cooling water for 'COOL-1' and 'COOL-2' was 10 °C at the inlet and 25 °C at the outlet.

The biomass to fuel efficiency (η_{btf}) and thermal efficiency (η_{th}) are described in Eqs. (14) and (15) respectively and followed the method mentioned in Lind et al. [39]. The biomass to fuel efficiency ignores additional power or heat inputs and outputs. The thermal efficiency includes net power transfers and net heat transfers. All heat transfers were considered regardless of their practical value if there was a

potential heat sink.

$$\eta_{btf} = \frac{\dot{Q}_{prod,i}}{\Sigma_j \dot{Q}_{biomass,j}} \tag{14}$$

where $\dot{Q}_{prod,i}$ and $\dot{Q}_{biomass,j}$ were the heating energy value Bio-SNG and glycerol respectively and were calculated by multiplying the lower heating value of the feedstock with the mass produced (Bio-SNG) or consumed (glycerol).

$$\eta_{th} = \frac{\Sigma_i \dot{Q}_{prod,i} + (P_{el}^- - P_{el}^+) + (\dot{Q}^- - \dot{Q}^+)}{\Sigma_i \dot{Q}_{biomass,j} + (P_{el}^+ - P_{el}^-) + (\dot{Q}^+ - \dot{Q}^-)} \tag{15}$$

where P_{el} is the electricity power required and $\dot{Q}$ was heat transfer rate. This equation considers whether energy is imported or exported denoted by superscript "−" or "+" respectively. The exported energy is any heat or electrical output produced in the process whereas imported energy is heat or electrical input required by the process and obtained externally e.g. from the grid. This method accounts for the net energy flows only such that a heat or electrical term can only appear once in the equation, either on the numerator or denominator. As such net exports appear on the numerator and net imports appear on the denominator. Lastly it treats all types of energy equally.

2.4. Plant sensitivity analysis

The two input variables of interest were S/C and pressure for the final plant design. The outlet variables of interest were the LHV of the Bio-SNG, inlet reformer temperature, CH_4 mole fraction in the reformate, and biomass to fuel efficiency and thermal efficiency. To compute these values, the mass flow rates of net Bio-SNG from the plant and of Bio-SNG for the furnace, Bio-SNG density and composition were obtained from the Aspen Plus calculations. The minimum inlet temperature to the reformer at each pressure had to be at least 463 K to satisfy the minimum temperature for catalysts displaying activity in the SR reactions. The minimum temperature to produce steam for each pressure was used as the inlet temperature for steam to the reformer. For 1 atm, the steam required superheating to reach above 463 K. The steam that could be produced from H1 was always maximised as well as the maximum increase in temperature for water from H2 to ensure that minimum fuel was required.

3. Thermodynamic analysis

The Gibbs free energy of reactions involved in direct methanation has been plotted in Fig. 3. CO methanation had the lowest ΔG until 973 K. Both CO and CO_2 methanation had lower ΔG than the water gas shift until 973 K. As temperature increased, the rate of increase of the ΔG for both methanation reactions was more significant than that of the water gas shift. Consequently, at lower temperatures, methanation was more thermodynamically favourable than water gas shift, with CO
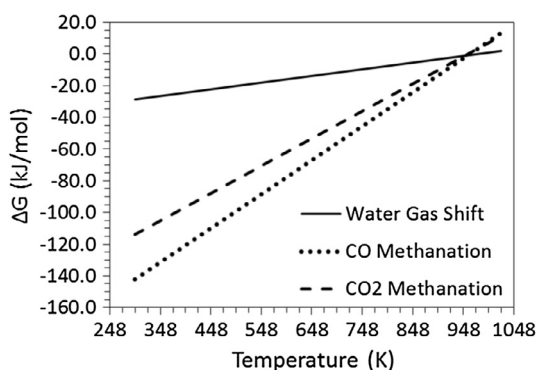
methanation being the strongest. As temperatures increased, both methanation reactions became less favourable whilst water gas shift became stronger in comparison. More hydrogen may be formed at equilibrium, consuming CO and reducing availability for CO methanation, but increasing the availability of CO_2 for methanation. This could explain why a reduction in methane was observed experimentally by [28] as they increased the temperature in their direct methanation reactions.

At higher temperatures, the loss of CH_4 was attributed to steam reforming of methane as well as the water gas shift reaction becoming more dominant than methanation. The latter was observed by Dieuzeide et al. [16] by studying reaction contributions.

The water gas shift and methanation reactions are both exothermic but CO and CO_2 methanation reactions have a more negative enthalpy of reaction and Gibbs free energy, when compared to the water gas shift at temperatures below 948 K (675 °C). The speed of the reactions and selectivity of the catalyst will be significant so the spontaneity of the reactions may not necessarily determine the actual distribution of products from glycerol methanation.

3.1. Isothermal methane and carbon formation

Fig. 4 describes the minimum S/C required to accomplish zero carbon at equilibrium under isothermal conditions. The minimum S/C varied for each temperature within the range of temperatures 400–1000 K (error ± 0.01 S/C or 0.03 water to glycerol ratio). The condition of zero carbon at equilibrium for Aspen Plus simulations was defined here as less than 1×10^{-5} mol hr^{-1} in the product gas stream. Areas to the left of the curve contained carbon as equilibrium product whereas areas to the right of the curve did not.

Starting from 550 K and descending to 400 K all the pressure dependent points for zero carbon converged, indicating that pressure had a minimum effect on the minimum S/C for zero carbon formation in this temperature range. At 600 K the points diverged, firstly with P1 (1 atm) and then with P4 (4 atm) at 650 K. The largest range occurred at 750 K with P30 (30 atm) requiring an S/C of 0.96 and P1 requiring an S/C of 1.14. All points except P1 converge again at 900 K before diverging again at 950 K. Between 600 K and 800 K increasing pressure reduces the S/C required for zero carbon formation. Above 850 K this trend is reversed. Adhikari et al. [14] reported a S/C of at least 1 was required to reduce carbon to zero at 800 K and 900 K and a S/C between 1 and 2 for 700 K and 600 K. The results within Fig. 4 fall within these boundaries. Dieuzeide and Amadeo [16] reported reductions in carbon formation at elevated pressures below 900 K and the reverse above 900 K. This manifests in the requirement for smaller S/C for zero carbon formation below 900 K at elevated pressures and larger S/C above 900 K at elevated pressures.

Fig. 5 describes the change in theoretical maximum CH_4 with changing reformer temperature at different pressures and at the

Fig. 3. Variation in Gibbs free energy with temperature of the key reactions in for direct methanation of glycerol under ideal conditions.
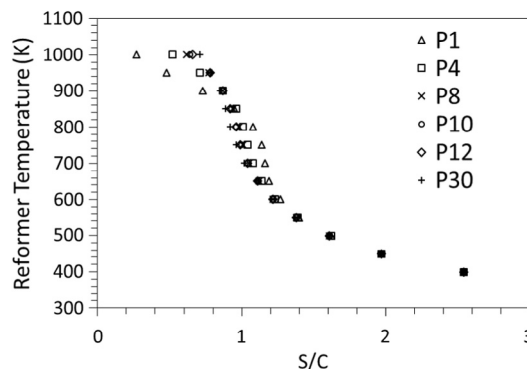
Fig. 4. Carbon product boundaries for pressures of 1, 4, 8 and 10 atm (P1-P10) under the IDEAL property method where S/C is steam to carbon ratio. Area on the left of the curves indicates solid C as significant equilibrium product.
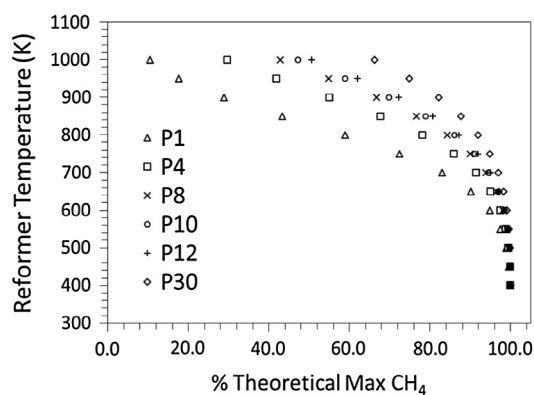
Fig. 5. Percentage maximum of theoretical CH$_4$ yield at the minimum S/C for zero carbon formation under the IDEAL property method.

Fig. 7. Property method sensitivity for the minimum S/C to produce negligible carbon at P1 and P8 for PENG.

minimum S/C ratio for zero carbon. The CH$_4$ yield is expressed as the percentage ratio of the Aspen Plus-calculated equilibrium CH$_4$ yield to the stoichiometric maximum, according to reaction Eq. (4).

As reformer temperature increased, less of the glycerol converted to CH$_4$ and more converted to H$_2$. Additionally at the minimum S/C for zero carbon formation, as expected, the maximum CH$_4$ was produced as increasing the S/C was found to favour hydrogen production rather than CH$_4$ production [14]. Dieuzeide and Amadeo mentioned that the maximum H$_2$ yield with temperature tended towards higher temperatures at increased pressures [16]. The same was true for CH$_4$ production. For example, at 1000 K the maximum CH$_4$ yield under 1 atm was 10%, rising to 30%, 42% and 47%, 50% and 66% for P4, P8, P10, P12, and P30 (4–30 atm) respectively. Whilst increasing the pressure to 30 atm was significant at 1000 K, less methane yield was gained when observing the pressure effect at low temperatures. This can be seen in Fig. 6 which shows more detail in the region of 80–100% of theoretical maximum CH$_4$ of 1.75 mol per mol of glycerol. Note that 86% of the theoretical maximum CH$_4$ yield would correspond to just half the carbon content of the glycerol feed converting to the intended CH$_4$ product.

At 600 K, increasing the pressure from 1 to 4 atm improved the methane yield by 2.5%, but increasing further to 8, 10, 12 and 30 atm increased the yield an additional 0.8, 0.2, 0.1 and 0.5%. At 600 K, it would be advantageous to increase the reformer pressure to at least 8 atm, but beyond this, increasing pressure to 30 atm only yielded a 0.7% increase of the theoretical maximum methane in addition to the 3.3% by increasing the pressure from 1 to 8 atm. The higher the temperature, the more worthwhile it was to increase the pressure to 30 atm to maximise methane yield.

When operating below the temperature range of 500 K, maintaining an operating pressure of 1 atm was sufficient to achieve a yield of 99%
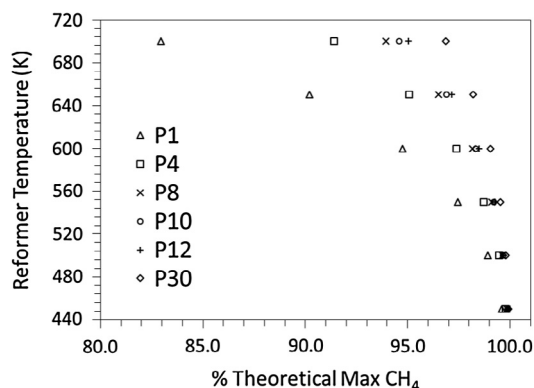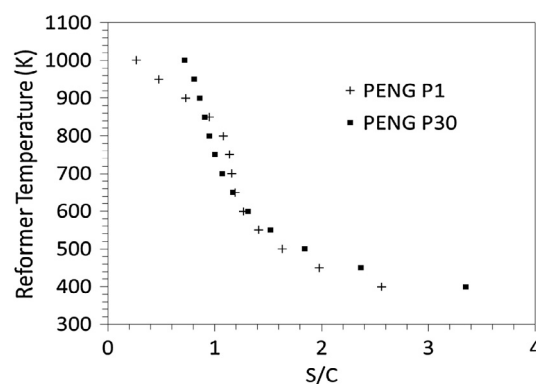
of the theoretical maximum methane under ideal conditions. To maintain this yield at 600 K, the pressure would need to increase to 30 atm. This revealed very high sensitivity of the CH$_4$ yield to temperature.

An integral consideration is the minimum temperature for conventional methanation catalysts at 463 K (190 °C). Based on the results in Figs. 5 and 6, maintaining a reformer temperature within the region of 463–600 K at pressure of 8 atm would be desirable to achieve conditions appropriate for the current generation of commercial methanation catalysts, and a low enough temperature to enable the highest methane yields. From Fig. 4, at 600 K an S/C of at least 1.2 and at 450 K of at least 2.0 would be required to minimise carbon equilibrium product and therefore maximise the feed carbon that could be converted to CH$_4$.

3.2. Property methods sensitivity

The effect of the property method at 1 and 8 atm on the minimum S/C for zero carbon product during glycerol steam reforming is shown in Fig. 7.

Property methods IDEAL, UNIQUAC and NRTL produced identical results where carbon product's sensitivity to S/C and reformer temperature was concerned.

Above 650 K the choice of property method had a negligible impact on the performance of glycerol steam reforming. At and below 600 K for P1 (1 atm) and 650 K for P30 (30 atm), the points began to diverge away from the ideal for PENG and NRTL-RK. Fig. 7 shows the results for PENG at 1 and 30 atm. At 30 atm the S/C required for zero carbon was larger than at 1 atm. As temperatures decreased, the S/C required to maintain zero carbon also increased. PENG and NRTL-RK property methods went against the IDEAL trend that increasing pressure below 900 K slightly reduced carbon product. The pressure effect was not observed by property methods relying on the ideal properties relationship (see Fig. 8.).

PENG and NRTL-RK do not depend upon the ideal gas law for their vapour phase equation of state calculations whereas IDEAL, UNIQUAC and NRTL do. PENG and NRTL-RK estimated greater steam to carbon ratios required to produce near zero solid carbon formation at temperatures below 700 K. Based on the results and the method from Carlson [33] the NRTL property method was chosen for the plant design.

There was little to no variance in the CH$_4$ yield at point of zero carbon when varying property methods. The PENG equation of state method and NRTL-RK activity coefficient method produced the same results as the IDEAL method for predicting CH$_4$ production by glycerol steam reforming when minimising Gibbs free energy under constant pressures and temperatures. Experimental data is required to validate the property methods.

Fig. 6. Percentage maximum of theoretical CH$_4$ yield at the minimum S/C for zero carbon formation under the IDEAL property method between 420 and 720 K.
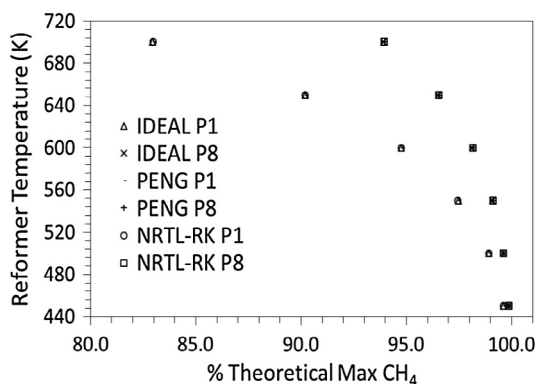
Fig. 8. Property method sensitivity for the CH$_4$ yield expressed as % theoretical maximum CH$_4$ for P1 (1 atm) and P8 (8 atm).

3.3. Adiabatic temperatures and vapour fraction

For direct methanation of glycerol, the process is mildly exothermic when compared to CO or CO$_2$ methanation, designated by the less negative enthalpy change in Eq. (2) when compared to the strongly negative ΔH of Eqs. (4) and (5). Consequently, the reactor would require cooling to maintain isothermal conditions. In practice, maintaining a constant temperature in a reactor housing exothermic reactions is difficult and requires accurate heat transfer controls. For a mildly exothermic reactor such as one carrying out direct methanation of glycerol, it is more practical and cheaper to operate the reactor without inner cooling, therefore the plant model in this work used adiabatic conditions in the reformer.

The minimum temperature for total vaporisation (vapour fraction = 1) of a water and glycerol mixture can be calculated in Aspen Plus, using the binary mixing analysis mode. The results are depicted in Fig. 9 at 8 atm. With a S/C of 2 the minimum vaporisation temperature was 576 K and S/C of 3 required 560 K creating a range of useful temperatures for the minimum vaporisation of 560–576 K for any S/C in between 2 and 3.

When the minimum temperatures of vaporisation were used in a steam reforming process for methane production in an adiabatic reactor, the outlet reformer temperatures were greater than 700 K. This is above the optimal temperature to achieve maximum methane production and is a result of the exothermic nature of methanation. To reduce the temperature of operation, the temperature of the inlet feed of glycerol and water can be reduced. Consequently, the vapour fraction of the inlet stream will also be below 1 representing a liquid vapour mix of glycerol-water feed. Alternatively generating steam and combining it with glycerol that is below its dew point will have the same effect. As a
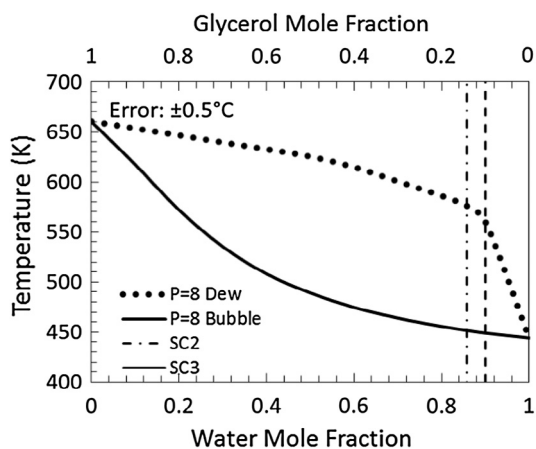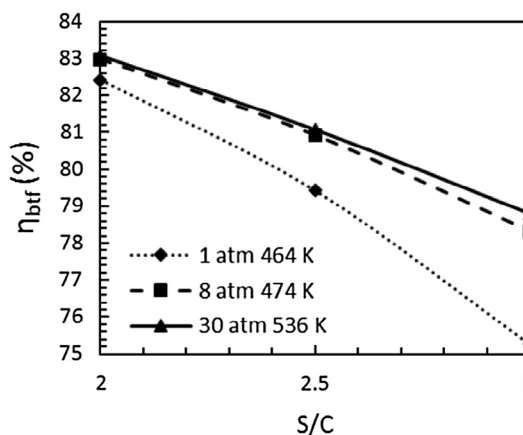
Fig. 10. Biomass to fuel efficiency versus steam to carbon ratio at pressures 1–30 atm with reformer inlet temperatures.

result, the glycerol will become partially vaporised in the reformer and as methanation takes place, the heat generated is used up to further vaporise the glycerol and prevent temperatures increasing above 700 K. This method of limiting reformer temperatures in exothermic reactors has been used previously in autothermal reforming (ATR). The method has been demonstrated experimentally by Liu et al. [40] using a nebuliser with an initial energy input to initiate partial oxidation and steam reforming and by Rennard et al. [41,42]. In the present process design, instead of the exothermic oxidation reactions driving the endothermic steam reforming, it is the exothermicity of the methanation reaction that is reined in.

4. Adiabatic GLT-SR plant

The impact of steam to carbon ratio and pressure on the biomass to fuel efficiency and inlet temperature can be seen in Fig. 10. As the S/C increased the efficiency was reduced at all pressures. This corresponded to an increase in the energy required to produce steam due to the increased mass of water as S/C increased. As more energy was needed, more of the Bio-SNG was re-routed to the furnace, reducing the net Bio-SNG produced and reducing the biomass to fuel efficiency. For a given S/C, efficiency increased with increasing pressure, this was related to conditions in the liquid glycerol and saturated steam mixer prior to the reformer. At the higher pressure, the saturated steam temperature at the mixer inlet resulted in the mixer outlet's glycerol/water mixture of vapour fraction lower than 1 with a temperature that exceeded the minimum for catalyst activation (463 K). This temperature became the reformer's inlet temperature, and is shown in the legend of Fig. 10 for pressures 8 and 30 atm (475 K and 536 K). In contrast at 1 atm, the saturated steam temperature at the mixer inlet would have resulted in an outlet mixer temperature lower than the minimum for reformer catalyst activation, thus necessitating an extra heat duty for superheating steam prior to the mixer to reach just above the minimum reformer catalyst temperature, as shown Fig. 10′s legend (1 atm, 464 K).

Increasing the pressure above 1 atm improved the efficiency of the process at higher steam to carbon ratios.

The outlet temperature of the reformer as varying with steam to carbon ratio at different pressures is plotted in Fig. 11. At higher steam to carbon ratios the outlet reformer temperature reduced.

The pressure of 8 atm produced the lowest outlet reformer temperatures whereas 1 atm had the highest outlet reformer temperatures. Increasing the pressure reduced the vapour fraction at the inlet but also increased the inlet reformer temperature as mentioned earlier. The reduced vapour fraction allowed more energy from exothermic reactions to be utilised for vaporising the water and glycerol, reducing the outlet reformer temperature. However, this was mitigated by increasing the inlet temperature to the reformer. For this reason, increasing the

Fig. 9. Vapour phase diagram for glycerol water mixtures at 8 atm.
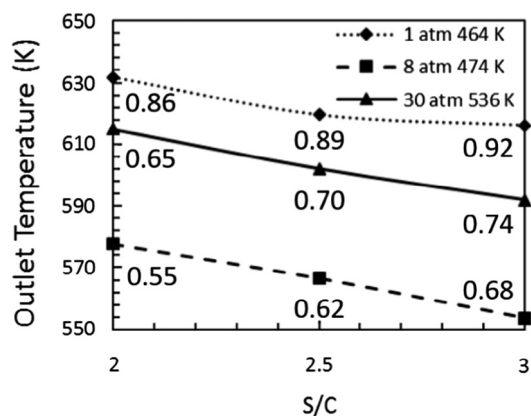
Fig. 11. Outlet temperature versus steam to carbon ratio at pressures 1, 8, and 30 atm and change in inlet vapour fraction with S/C at different pressures. Vapour fraction at each temperature and S/C is noted at each point to two decimal places.

pressure from 8 atm to 30 atm increased the outlet reformer temperature even though the inlet vapour fraction at 30 atm was lower.

From this modelled data operating at 8 atm provided the benefits of higher biomass to fuel efficiencies than at 1 atm, via lower increases in temperature at the reformer outlet than 30 atm and achieving the minimum inlet temperature for catalyst operation.

High pressure steam recovery allowed up to 21% of the high-pressure steam to be re-generated from the steam reformer output stream. Flue gas recirculation (FGR) recycled 20% of the exhaust gas to the furnace to maintain an outlet temperature of 1313 °C (1591.15 K). The furnace required 17% of the total Bio-SNG as fuel for the boiler, when the furnace operated at an efficiency of 90% and energy transfer to the steam operated at 81% as calculated. The high and low-pressure steam produced were not superheated. Overall, 1 kg of glycerol produced 0.91 kg total Bio-SNG with a requirement of 1.18 kg of non-superheated steam at 8 atm under this GLT-SR process. The net Bio-SNG produced was $0.763 \, kg \, hr^{-1} \, kg^{-1}$ glycerol as $0.147 \, kg \, hr^{-1}$ Bio-SNG was required for heating the GLT-SR process, assuming a combined boiler and furnace efficiency of 90%.

4.1. Bio-SNG composition

The composition and characteristics of the simulated Bio-SNG were in between landfill gas and biogas from anaerobic digestion (A.D.) as shown in Table 1. As a consequence, Bio-SNG was not suitable for grid injection or as vehicle fuel without further gas upgrading (CO_2 separation). However the Bio-SNG was suitable for combustion on site for heat or in a combined heat and power engine. As the pure glycerol feed contained no H_2S nor Si, combustion of the Bio-SNG will have less corrosive or fouling effects on the machinery than landfill or biogas. On the other hand, this work focuses on pure glycerol as feed. If crude glycerol were used, there would most certainly be an effect on the final composition of the Bio-SNG due to residues from common transesterification catalysts and other contaminants, as shown by studies utilising crude glycerol for syngas production [21].

The heating value of Bio-SNG decreased when produced at 1 atm because of the increase in mole fraction of hydrogen. At 8 atm the hydrogen mole fraction is 4% whereas at 1 atm it is 20%. Increased hydrogen content leads to a lower density per Nm³. Operating at 30 atm produced nearly identical gas composition as 8 atm. To produce a gas with the highest heating value and CH_4 mole fraction, the process should operate at 8 atm.

4.2. Energy balance and analysis

The LHV of Bio-SNG was calculated as $16.7 \, MJ \, kg^{-1}$. The LHV of glycerol has been recorded as $16.0 \, MJ \, kg^{-1}$ [44] but Aspen plus uses

Table 1
Comparison of bio-SNG biogas and landfill gas. Landfill gas and Biogas data are taken from Clark et al. [43].

	Units	Bio-SNG (1 atm, 464 K, S/C 2)	Bio-SNG (8 atm, 474 K, S/C 2)	Landfill gas	Biogas from A.D
Methane	Vol%	41	55	45	65
Hydrogen	Vol%	21	4	0–3	0
Hydrocarbons C2+	Vol%	–	–	0	0
Hydrogen Sulphide	ppm	–	–	0–100	0–4000
Carbon Dioxide	Vol%	38	41	15–40	30–40
Nitrogen	Vol%	–	–	5–40	0.2
Oxygen	Vol%	–	–	1	
Carbon Monoxide	Vol%	0	0	–	–
Ammonia	ppm	–	–	5	100
Water	Vol%	0	0	–	–
Chlorine (Cl⁻)	Mg/Nm³	–	–	20–200	0–5
HHV_G	MJ/kg	17.9	18.6	–	–
LHV_G	MJ/kg	16.0	16.7	12.3	20
Density	kg/Nm³	1.01	1.14	–	–
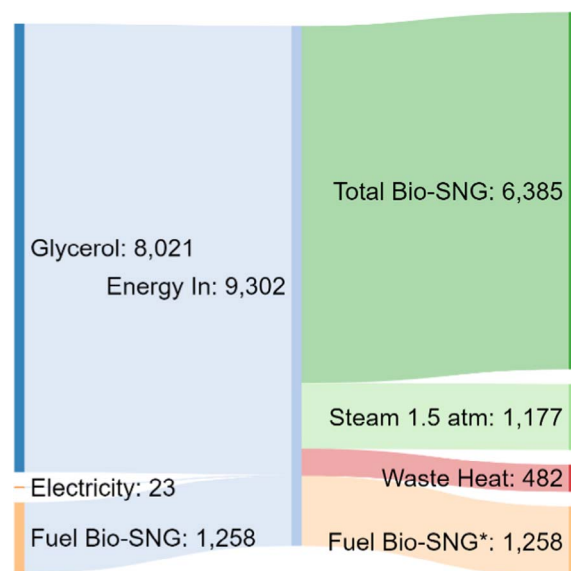
Fig. 12. Sankey diagram of the GLT-SR process at 8 atm. Flow is from left to right with the total system energy in the middle column. Fuel Bio-SNG is produced and used in the process and appears on the left and right side of the total system energy. Flow colours correspond to the same colour as their target node. (For interpretation of the references to colour in this figure legend, the reader is referred to the web version of this article.)

Table 2
Efficiency values for GLT-SR at 8 atm. Solid wood for Gasification values taken from Lind et al. [39]. Electrical efficiency and furnace boiler efficiency were 40% and 90% respectively and all values were calculated on an LHV basis.

Efficiency LHV based	GLT-SR for bio-SNG	Solid wood gasification for methane	GLT-SR for steam	GLT-SR for CHP
Biomass to Fuel η_{btf} (%)	83	63	73	66
Thermal η_{th} (%)	95	70	86	78

the value of 16.07. For every $kg \, hr^{-1}$ of glycerol converted, $15.3 \, MJ \, hr^{-1}$ of total Bio-SNG was produced and $2.6 \, MJ \, hr^{-1}$ required for the boiler resulting in 12.7 MJ of net Bio-SNG, in addition to 2.5 MJ of steam. Fig. 12 illustrates the energy inputs and outputs with Table 2

listing the associated biomass to fuel and thermal efficiencies. The power demand of the process was 23 MJ hr^{-1} and equated to less than 1% of the energy contained in the Bio-SNG.

Results for plant efficiency calculations are shown in Table 2. The η_{btf} was 83% for GLT-SR which was greater than solid wood gasification for methane production, which had a η_{btf} of 63% [39]. The η_{btf} was lower than 100% because some of the Bio-SNG was combusted in a furnace to convert water to steam. Nearly 17% of the total Bio-SNG produced was re-directed to the furnace and combusted with 10% excess air to provide heat for raising steam as shown in Fig. 2 by the RE-BG stream and represented by the Fuel Bio-SNG area in Fig. 12.

The thermal efficiency assumes that the heat from the low-pressure steam generation is useful. It does not account for the waste heat, which is heat lost from the condenser and in the flue gas, because this heat has no useful sink. Electricity demand is also accounted for in the thermal efficiency but because the electricity demand of the process is less than 0.5% of the energy contained in the glycerol by LHV, the impact on the efficiency is low. Consequently, the biomass to fuel efficiency is a good indicator of the GLT-SR process efficiency if the steam does not have a useful sink. As the steam is low pressure (1.5 bar) it will likely only have application in heating, ventilation and air-conditioning (HVAC) settings.

An important assumption is that these efficiencies treat energy equally and must be considered when comparing against a process that produces electricity. Furthermore, this does not account for the end use efficiency of the Bio-SNG, such as the efficiency of combustion in a boiler or CHP unit. Therefore, the conversion to steam or CHP was calculated as shown by Table 2.

If the Bio-SNG was intended to be used for steam production, a furnace and boiler efficiencies of 90% can be assumed as with the GLT-SR process. In a similar way, utilising the Bio-SNG in a CHP for steam and electricity generation, we can assume a combined efficiency of 80%. The η_{btf} reduces by 8.4% when the product is steam and 16.8% when the product is electricity and steam from a CHP. The η_{th} reduces by 7.1 and 14.2% for steam generation, compared to heat and power, respectively.

Decreasing furnace efficiency is expected to occur over time unless it is maintained. The results of a sensitivity analysis to explore the effects of reducing the heat transfer efficiency are shown in Table 3 when Bio-SNG is treated as the product with no further conversion. For every 10% decrease in efficiency for the heat transfer in the furnace and boiler a reduction in η_{th} and η_{btf} of 1.6% occurs. This is equivalent to 126 MJ hr^{-1} of Bio-SNG. This manifests in the increase in Bio-SNG required for the furnace, diverting energy away from the net Bio-SNG which could be used to offset natural gas. Maintaining the heat transfer efficiency through good boiler and furnace maintenance will contribute to maximising the Bio-SNG potential. Additionally, upgrading from an old and less efficient boiler to a more modern and more efficient boiler could increase the net Bio-SNG product from 2 to 9%.

The soybean biodiesel life cycle analysis by Pradhan et al. [35] describes the energy and resource requirements of each stage of the soybean biodiesel process. To compare like for like, the embodied energy from Pradhan et al. is compared to the embodied energy of the net Bio-SNG of the present study on a LHV basis. In this process, natural gas

Table 3
Effects of decreasing furnace efficiency on required Bio-SNG.

Furnace efficiency (%)	Percentage of total Bio-SNG required for Furnace (%)	η_{th} (%)	η_{btf} (%)
100	16	94	83
90	18	92	81
80	20	91	79
70	21	89	78
60	23	88	76
50	25	86	74
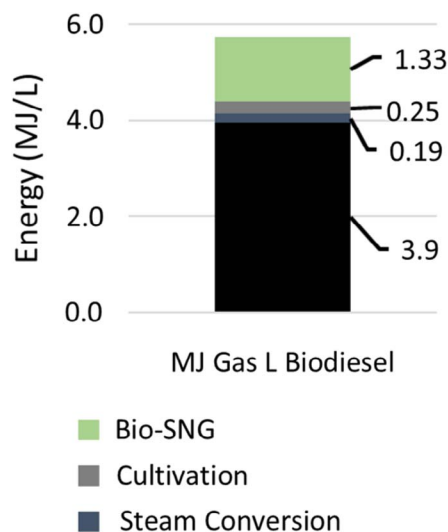
Fig. 13. Breakdown of the natural gas embodied energy requirements of per litre of soybean biodiesel, including co-products. From top to bottom, Bio-SNG, Cultivation, Steam Conversion, Soybean Crushing.

was combusted for heat to crush soybeans.

Producing Bio-SNG from glycerol can offset 30% (1.33 MJ L$_{biodiesel}$$^{-1}$) of the total natural gas required (4.40 MJ L$_{biodiesel}$$^{-1}$) to produce one litre of soybean biodiesel and additional co-products, as shown in Fig. 13. The total natural gas requirements for soybean biodiesel are composed of: soybean cultivation at 0.25 MJ L$_{biodiesel}$$^{-1}$, soybean crushing at 3.9 MJ L$_{biodiesel}$$^{-1}$ and steam production for biodiesel conversion at 0.19 MJ L$_{biodiesel}$$^{-1}$.

In this scenario, it was assumed that the natural gas for crushing and steam production were the only areas of natural gas demand that could be substituted by the Bio-SNG produced from an on-site GLT-SR process. Using the Bio-SNG for cultivation would involve transportation of the Bio-SNG, requiring additional compression. The total life cycle energy for soybean biodiesel was 17.8 MJ L$_{biodiesel}$$^{-1}$ as calculated by [35]. Using their life cycle energy factors, the total embodied energy was calculated as 14.8 MJ L$_{biodiesel}$$^{-1}$. Bio-SNG produced from GLT-SR has the potential to offset 9% of the total embodied energy required to produce soybean biodiesel if it is used on site to substitute natural gas to provide heat and steam for the crushing process.

5. Conclusions

A thermodynamic analysis of the direct methanation of pure glycerol by steam reforming was carried out. The minimum steam to carbon ratios for zero carbon formation at different temperatures and pressures were determined and complete conversion of glycerol to a medium methane content gas was observed.

Re-routing a fraction o the Bio-SNG to produce steam resulted in a thermally self-sufficient process with a negligible power demand and an overall positive net energy gain. It was calculated that the Bio-SNG produced at 8 atm and S/C 2 could offset up to 30% of the natural gas embodied energy requirement of soybean biodiesel production, or 8.9% of the total embodied energy requirement for soybean biodiesel, could be offset by Bio-SNG.

The potential benefits for the biodiesel refinery include: a reduction in carbon emissions, taking advantage of renewable subsidies, and waste reduction. If no other beneficial use for the glycerol can be found, this process offers a useful alternative to incineration and disposal, avoiding associated environmental hazards and fees.

The authors conclude that the process is feasible in terms of energy. Experimental work is required to validate the modelled results and this work acts as justification for more in depth studies in the process of low

temperature steam reforming of glycerol to produce bio-SNG.

Appendix A. Supplementary material

Supplementary data associated with this article can be found, in the online version, at http://dx.doi.org/10.1016/j.enconman.2018.01.031.

References

[1] OECD. OECD-FAO agricultural outlook 2014. OECD Publishing; 2014. http://dx.doi.org/10.1787/agr_outlook-2014-en.
[2] OECD, FAO. OECD-FAO agricultural outlook 2016; 2016. http://dx.doi.org/10.1787/19991142.
[3] Ciriminna R, Pina C Della, Rossi M, Pagliaro M. Understanding the glycerol market. Eur J Lipid Sci Technol 2014;116:1432–9. http://dx.doi.org/10.1002/ejlt.201400229.
[4] DEFRA. AQ06 (08) Additional Guidance from Defra and the Welsh Assembly Government - June 2008, vol. 6; 2008.
[5] He(Sophia) Q, McNutt J, Yang J. Utilization of the residual glycerol from biodiesel production for renewable energy generation. Renew Sustain Energy Rev 2017;71:63–76. http://dx.doi.org/10.1016/j.rser.2016.12.110.
[6] Schwengber CA, Alves HJ, Schaffner RA, da Silva FA, Sequinel R, Bach VR, et al. Overview of glycerol reforming for hydrogen production. Renew Sustain Energy Rev 2016;58:259–66. http://dx.doi.org/10.1016/j.rser.2015.12.279.
[7] Wu YJ, Li P, Yu JG, Cunha AF, Rodrigues AE. Progress on sorption-enhanced reaction process for hydrogen production. Rev Chem Eng 2016;32:271–303.
[8] Shokrollahi Yancheshmeh M, Radfarnia HR, Iliuta MC. High temperature CO2 sorbents and their application for hydrogen production by sorption enhanced steam reforming process. Chem Eng J 2016;283:420–44. http://dx.doi.org/10.1016/j.cej.2015.06.060.
[9] Tippawan P, Thammasit T, Assabumrungrat S, Arpornwichanop A. Using glycerol for hydrogen production via sorption-enhanced chemical looping reforming: Thermodynamic analysis. Energy Convers Manage 2016;124:325–32. http://dx.doi.org/10.1016/j.enconman.2016.07.018.
[10] Freitas ACD, Guirardello R. Comparison of several glycerol reforming methods for hydrogen and syngas production using Gibbs energy minimization. Int J Hydrogen Energy 2014;39:17969–84. http://dx.doi.org/10.1016/j.ijhydene.2014.03.130.
[11] Rodrigues A, Bordado JC, dos Santos RG. Upgrading the glycerol from biodiesel production as a source of energy carriers and chemicals—a technological review for three chemical pathways. Energies 2017;10:1–35. http://dx.doi.org/10.3390/en10111817.
[12] Coronado I, Stekrova M, Reinikainen M, Simell P, Lefferts L, Lehtonen J. A review of catalytic aqueous-phase reforming of oxygenated hydrocarbons derived from biorefinery water fractions. Int J Hydrogen Energy 2016;41:11003–32. http://dx.doi.org/10.1016/j.ijhydene.2016.05.032.
[13] Bagnato G, Iulianelli A, Sanna A, Basile A. Glycerol production and transformation: a critical review with particular emphasis on glycerol reforming reaction for producing hydrogen in conventional and membrane reactors. Membranes (Basel) 2017;7. http://dx.doi.org/10.3390/membranes7020017.
[14] Adhikari S, Fernando S, Gwaltney S, Filipto S, Markbricka R, Steele P, et al. A thermodynamic analysis of hydrogen production by steam reforming of glycerol. Int J Hydrogen Energy 2007;32:2875–80. http://dx.doi.org/10.1016/j.ijhydene.2007.03.023.
[15] Rossi CCRS, Alonso CG, Antunes OaC, Guirardello R, Cardozo-Filho L. Thermodynamic analysis of steam reforming of ethanol and glycerine for hydrogen production. Int J Hydrogen Energy 2009;34:323–32. http://dx.doi.org/10.1016/j.ijhydene.2008.09.071.
[16] Dieuzeide ML, Amadeo N. Thermodynamic analysis of glycerol steam reforming. Chem Eng Technol 2010;33:89–96. http://dx.doi.org/10.1002/ceat.200900260.
[17] Chen H, Ding Y, Cong NT, Dou B, Dupont V, Ghadiri M, et al. A comparative study on hydrogen production from steam-glycerol reforming: thermodynamics and experimental. Renew Energy 2011;36:779–88. http://dx.doi.org/10.1016/j.renene.2010.07.026.
[18] Wang X, Wang N, Li M, Li S, Wang S, Ma X. Hydrogen production by glycerol steam reforming with in situ hydrogen separation: a thermodynamic investigation. Int J Hydrogen Energy 2010;35:10252–6. http://dx.doi.org/10.1016/j.ijhydene.2010.07.140.
[19] Wang X, Li S, Wang H, Liu B, Ma X. Thermodynamic analysis of glycerin steam reforming. Energy Fuels 2008;22:4285–91. http://dx.doi.org/10.1021/ef800487r.
[20] Silva JM, Soria MA, Madeira LM. Thermodynamic analysis of Glycerol Steam Reforming for hydrogen production with in situ hydrogen and carbon dioxide separation. J Power Sources 2015;273:423–30. http://dx.doi.org/10.1016/j.jpowsour.2014.09.093.
[21] Sabio E, Álvarez-Murillo A, González JF, Ledesma B, Román S. Modelling the composition of the gas obtained by steam reforming of glycerine. Energy Convers Manage 2017;146:147–57. http://dx.doi.org/10.1016/j.enconman.2017.03.068.
[22] Veiga S, Bussi J. Steam reforming of crude glycerol over nickel supported on activated carbon. Energy Convers Manage 2017;141:79–84. http://dx.doi.org/10.1016/j.enconman.2016.04.103.
[23] Zarei Senseni A, Meshkani F, Seyed Fattahi SM, Rezaei M. A theoretical and experimental study of glycerol steam reforming over Rh/MgAl2O4catalysts. Energy Convers Manage 2017;154:127–37. http://dx.doi.org/10.1016/j.enconman.2017.10.033.
[24] Veiga S, Faccio R, Segobia D, Apesteguía C, Bussi J. Hydrogen production by crude glycerol steam reforming over Ni–La–Ti mixed oxide catalysts. Int J Hydrogen Energy 2017;42:30525–34. http://dx.doi.org/10.1016/j.ijhydene.2017.10.118.
[25] Wang S, Wang Q, Song X, Chen J. Dry autothermal reforming of glycerol with in situ hydrogen separation via thermodynamic evaluation. Int J Hydrogen Energy 2017;42:838–47. http://dx.doi.org/10.1016/j.ijhydene.2016.09.103.
[26] Schubert M, Mu JB. Continuous hydrothermal gasification of glycerol mixtures: autothermal operation, simultaneous salt recovery, and the effect of K3PO4 on the catalytic gasification. J Supercrit Fluids 2014;95:4–15. http://dx.doi.org/10.1016/j.supflu.2014.09.011.
[27] Meyer H, Hill VL, Flowers A, Happel J, Hnatow M. Direct methanation - a new method of converting synthesis gas to substitute natural gas. 1976. p. 109–15.
[28] Mai HI, Amawaki MY, Xiaohong LI. Direct synthesis of methane from glycerol by using silica-modified nickel catalyst. 2017; 60: p. 311–21.
[29] Chen H, Zhang T, Dou B, Dupont V, Williams P, Ghadiri M, et al. Thermodynamic analyses of adsorption-enhanced steam reforming of glycerol for hydrogen production. Int J Hydrogen Energy 2009;34:7208–22. http://dx.doi.org/10.1016/j.ijhydene.2009.06.070.
[30] Haldor Topsoe. PK-7R 2017:1. https://www.topsoe.com/products/pk-7r [accessed 12.12.17].
[31] Zhang B, Tang X, Li Y, Xu Y, Shen W. Hydrogen production from steam reforming of ethanol and glycerol over ceria-supported metal catalysts. Int J Hydrogen Energy 2007;32:2367–73. http://dx.doi.org/10.1016/j.ijhydene.2006.11.003.
[32] Stangeland K, Kalai D, Li H, Yu Z. CO 2 methanation: the effect of catalysts and reaction conditions. Energy Procedia 2017;105:2022–7. http://dx.doi.org/10.1016/j.egypro.2017.03.577.
[33] Carlson EC. Don't gamble with physical properties. Chem Eng Process 1996:35–46.
[34] Annesini MC, Piemonte V, Turchetti L. Carbon formation in the steam reforming process: a thermodynamic analysis based on the elemental composition. Chem Eng Trans 2007;11:1–30. http://dx.doi.org/10.1017/CBO9781107415324.004.
[35] Pradhan A, Shrestha DS, Mcaloon A, Yee W, Haas M, Duffield JA. Energy life cycle assessment of soybean biodiesel revisited. Am Soc Agric Biol Eng 2011;54:1031–9.
[36] Huo H, Wang M, Bloyd C, Putsche V. Life-cycle assessment of energy use and greenhouse gas emissions of soybean-derived biodiesel and renewable fuels. Environ Sci Technol 2009;43:750–6. http://dx.doi.org/10.1021/es8011436.
[37] Ashrae. HEATING EQUIPMENT AND COMPONENTS - Boilers. Ashrae Handb. -HVAC Syst. Equip., American Society of Heating, Refrigerating and Air-Conditioning Engineers, 2016; 2016.
[38] Liuzzo G, Verdone N, Bravi M. The benefits of flue gas recirculation in waste incineration. Waste Manage 2007;27:106–16. http://dx.doi.org/10.1016/j.wasman.2006.01.002.
[39] Lind F, Heyne S, Johnsson F. What is the efficiency of a biorefinery. In: Sandén B, Pettersson K, editors. Syst. Perspect. Biorefineries. 3.1. Göteborg: Chalmers University of Technology; 2014. p. 106–20.
[40] Liu Y, Farrauto R, Lawal A. Autothermal reforming of glycerol in a dual layer monolith catalyst. Chem Eng Sci 2013;89:31–9. http://dx.doi.org/10.1016/j.ces.2012.11.030.
[41] Rennard DC, Kruger JS, Schmidt LD. Autothermal catalytic partial oxidation of glycerol to syngas and to non-equilibrium products. ChemSusChem 2009;2:89–98. http://dx.doi.org/10.1002/cssc.200800200.
[42] Rennard DC, Kruger JS, Michael BC, Schmidt LD. Long-time behavior of the catalytic partial oxidation of glycerol in an autothermal reactor. Ind Eng Chem Res 2010;49:8424–32. http://dx.doi.org/10.1021/ie100405h.
[43] Clark RH. Basic data on biogas composition; 2007. doi: ISBN 978-91-85207-7.
[44] Czernichowski A, Czernichowski J, Czernichowski C. Glycerol conversion into clean and renewable liquid fuel; 2010.